Intense Laser Pulse Propagation and Stability in Partially Stripped Plasmas

P. Sprangle, E. Esarey, and B. Hafizi*
Beam Physics Branch, Plasma Physics Division, Naval Research Laboratory, Washington, D.C. 20375
(Received 7 April 1997)

In a partially stripped plasma the presence of bound electrons can significantly alter the propagation and stability of intense laser pulses. In the presence of both free and bound electrons, an atomic modulation instability develops that can have a growth rate substantially higher than either the conventional relativistic modulational instability or the forward Raman instability. In addition, the filamentation instability can be significantly enhanced by bound electrons while the backward Raman instability is unaffected. [S0031-9007(97)03730-7]

PACS numbers: 52.40.Nk

The propagation of intense laser pulses in plasmas is relevant to a wide range of applications, such as x-ray lasers [1], laser fusion [2], laser-plasma accelerators [3,4], harmonic generation in plasmas and gases [5,6], and laser-plasma channeling [7–9]. In many experiments the ions are not fully stripped and hence the propagation medium consists of both free and bound electrons. We find that bound electrons can lead to an atomic modulation instability (AMI), which can dominate the conventional relativistic modulational instability (RMI) [10–12] and the forward Raman scattering (FRS) [12–14] instability. The AMI requires both free and bound electrons, i.e., the free electrons provide anomalous group velocity dispersion (GVD), whereas the bound electrons provide self-phase modulation. In addition, bound electrons can result in an atomic filamentation instability (AFI), which can dominate the conventional relativistic filamentation instability (RFI) [10–12].

The refractive index associated with an intense laser pulse in a partially stripped plasma is $\eta = 1 + \Delta\eta$, with $\Delta\eta = \eta_0 - 1 + \Delta\eta_p + \Delta\eta_{pw} + \Delta\eta_r + \Delta\eta_a$ and $|\Delta\eta| \ll 1$, where $\eta_0 \cong 1$ is the linear index associated with the bound (atomic) electrons, $\Delta\eta_p = -\omega_p^2/2\omega_0^2$ is the linear contribution from the free (plasma) electrons, $\Delta\eta_{pw} = \Delta\eta_p(\delta\eta_p/n_p)$ is the nonlinear contribution from the excited plasma wave, $\Delta\eta_r = -\Delta\eta_p a_0^2/4$ is the relativistic contribution from plasma electrons, and $\Delta\eta_a = \eta_2 I$ is the nonlinear contribution from the bound atomic electrons. In the above, $\omega_0 = 2\pi c/\lambda_0$ is the laser frequency, λ_0 is the laser wavelength, $\omega_p = (4\pi q^2 n_p/m)^{1/2}$ is the plasma frequency, n_p is the ambient plasma density, δn_p is the perturbed plasma density, a_0 is the normalized (unitless) peak amplitude of the laser vector potential, η_2 is the nonlinear refractive index associated with the bound electrons, and I is the time averaged laser intensity. For a linearly polarized laser beam $a_0^2 = 7.32 \times 10^{-19} \lambda_0^2[\mu\mathrm{m}] I[\mathrm{W/cm^2}]$.

Self-focusing of the laser pulse requires that the radial gradient of the refractive index be negative, i.e., $\partial\Delta\eta/\partial r < 0$. It can be shown that the condition for self-focusing is $(\pi r_0/\lambda_0)^2\ \Delta\eta_{r,a} \geq 1$, where r_0 is the laser spot size and $r_0^2\Delta\eta_{r,a}$ is proportional to the laser power. This implies that the refractive indices associated with the relativistic plasma $\Delta\eta_r$ and bound electrons $\Delta\eta_a$ can individually cause focusing of the laser pulse if certain critical power levels are exceeded [3,8–10,15–17]. For linearly polarized light with a Gaussian transverse profile, the critical powers for relativistic focusing in a plasma [3,16] and nonlinear focusing in a gas [9,17] are, respectively, $P_p = 2c(q/r_e)^2(\omega_0/\omega_p)^2$, and $P_a = \lambda_0^2/(2\pi\eta_0\eta_2)$, where $r_e = q^2/mc^2 = 2.82 \times 10^{-13}$ cm is the classical electron radius. The ratio of the critical powers can be much greater than unity and scales with laser frequency to the fourth power,

$$R = \frac{P_p}{P_a} = \frac{1.22 \times 10^{40}\eta_0\eta_2[\mathrm{cm^2/W}]}{\lambda_0^4[\mu\mathrm{m}]\, n_p[\mathrm{cm^{-3}}]}, \qquad (1)$$

where η_2 is proportional to the atomic gas density, n_a. For example, taking $\eta_2 \cong 10^{-19}$ cm^2/W for typical gases at STP, $n_p = n_a = 2.7 \times 10^{19}$ cm^{-3} and $\lambda_0 = 0.5$ μm, we find that $R \cong 720$ ($P_p = 2.8$ TW and $P_a = 3.9$ GW). In a partially stripped plasma, if $R \gg 1$, the bound electrons have a much greater effect on the focusing of the laser pulse than the free electrons.

The wave equation for a laser pulse propagating in a partially stripped plasma is $(\nabla^2 - c^{-2}\partial^2/\partial t^2)\mathbf{E} = 4\pi c^{-2}\partial\mathbf{J}_T/\partial t$, where $\mathbf{J}_T = \partial\mathbf{P}/\partial t + \mathbf{J}_p$ is the total current density, $\mathbf{E}$ is the laser electric field, $\mathbf{P}$ is the polarization field associated with the bound electrons, and $\mathbf{J}_p$ is the plasma current density. The polarization field can be expressed by $\mathbf{P} = [\chi^{(1)} + \chi^{(3)}(\mathbf{E}\cdot\mathbf{E})]\mathbf{E}$, where $\chi^{(1)}$ ($\chi^{(3)}$) is the linear (third order) susceptibility associated with the bound electrons. The time averaged refractive index of the bound electrons is $\eta = \eta_0 + \eta_2 I$, where $\eta_0 = (1 + 4\pi\chi^{(1)})^{1/2}$ is the linear index, $\eta_2 = 8\pi^2\chi^{(3)}/\eta_0^2 c$ is the nonlinear refractive index, and $I = (c/4\pi)\eta_0\langle\mathbf{E}\cdot\mathbf{E}\rangle$. For the expansion of the polarization field in powers of the field to be valid we require $I \ll (\eta_0 - 1)/\eta_2$, i.e., $a_0^2 \ll 7.32 \times 10^{-19}\lambda_0^2[\mu\mathrm{m}](\eta_0 - 1)/\eta_2[\mathrm{cm^2/W}]$.

Values of $\chi^{(3)}$ for partially stripped atoms are not commonly known but can be readily calculated. For the

 0031-9007/97/79(6)/1046(4)$10.00

purpose of estimating these values, we will assume the charge state is small compared to the atomic number and, therefore, $\chi^{(3)}$ for a partially stripped atom is expected to be within an order of magnitude of the neutral atom value. Near resonances, however, large changes in $\chi^{(3)}$ and $\chi^{(1)}$ can occur. The nonlinear susceptibility $\chi^{(3)}$ for an ionized atom can be estimated if the charge state is small compared to the atomic number and the optical frequency is far below any atomic resonance. The ratio of the nonlinear susceptibilities of the ionized atom to the neutral atom is $\chi_+^{(3)}/\chi^{(3)} \approx (U_\mathrm{I}/U_\mathrm{I}^+)^3$, where U_I is the ionization potential for the neutral atom and U_I^+ is the ionization potential for the ionized atom. As an example, for Xe gas, $U_\mathrm{I} = 12.1$ eV, $U_\mathrm{I}^+ = 21.2$ eV (for singly ionized state), and $\chi_+^{(3)}/\chi^{(3)} \cong 0.18$. It is important to note that the validity of the present analysis is not contingent on $\chi^{(3)}$ being accurately known. Our results are expressed in terms of the effective value of R, which is proportional to $\chi^{(3)}$ for a partially stripped atom, and examples are given for a wide range of R. The assumption that the average charge state is small compared to the atomic number implies that the intensity is lower than the threshold for ionization of the next charge state and the laser pulse length is sufficiently short so as to avoid further electron collisional ionization.

It is convenient to write the wave equation in terms of the normalized vector potential $\mathbf{a}$, and to use the Coulomb gauge, $\nabla \cdot \mathbf{a} = 0$. The radiation field is assumed to consist of plane waves polarized in the x direction of the form $\mathbf{a} = (a_p + a_+ + a_-)\hat{\mathbf{e}}_x$ where a_p denotes the pump, $a_\pm$ are the anti-Stokes and Stokes sidebands, and $|a_\pm| \ll |a_p|$. The pump wave is represented by $a_p = (a_0/2)\exp[i(k_0 z - \omega_0 t)] + \text{c.c.}$, while the sidebands are given by $a_+ = (\hat{a}_+/2)\exp\{i[(k_0 + k)z + k_\perp y - (\omega_0 + \omega)t]\} + \text{c.c.}$, and $a_- = (\hat{a}_-/2) \times \exp\{i[(k_0 - k)z - k_\perp y - (\omega_0 - \omega^*)t]\} + \text{c.c.}$, where k_0 and ω_0 are the wave number and frequency of the pump, k, $k_\perp$, and ω are the real axial wave number, real transverse wave number, and complex frequency of the sidebands, and $*$ denotes the complex conjugate. The amplitude of the pump and sidebands are real and given by a_0 and $\hat{a}_\pm$, respectively. The plasma current density, correct to third order in $\mathbf{a}$, is [3,14] $\mathbf{J}_p = q n_p c(1 + \delta n_p/n_p - \mathbf{a}\cdot\mathbf{a}/2)\mathbf{a}$, where the term proportional to $\mathbf{a}\cdot\mathbf{a}$ is due to relativistic changes in the electron mass. The perturbed plasma density [3,14] is given by $(\partial^2/\partial t^2 + \omega_p^2)\delta n_p/n_p = (c^2/2)\nabla^2(\mathbf{a}\cdot\mathbf{a})$, where $\nabla^2 = \partial^2/\partial y^2 + \partial^2/\partial z^2$. Substituting $\mathbf{J}_p$, together with the polarization field in terms of $\mathbf{a}$, into the wave equation yields

$$\left(\nabla^2 - \eta_0^2 c^{-2}\frac{\partial^2}{\partial t^2} - k_p^2\right)\mathbf{a} = k_p^2\frac{\delta n_p}{n_p}\mathbf{a} - \frac{k_p^2}{2}\left\{(\mathbf{a}\cdot\mathbf{a})\mathbf{a} - R\omega_0^{-4}\frac{\partial}{\partial t}\left[\left(\frac{\partial\mathbf{a}}{\partial t}\cdot\frac{\partial\mathbf{a}}{\partial t}\right)\frac{\partial\mathbf{a}}{\partial t}\right]\right\}, \tag{2}$$

where $k_p = \omega_p/c$ and R is effective value in a partially stripped plasma.

The nonlinear dispersion relation for a linearly polarized pump wave is $\eta_0^2\omega_0^2/c^2 - k_0^2 - k_p^2 + k_p^2[\alpha_0 a_0^2 + (3/8)Ra_0^2] = 0$, where R is given by Eq. (1) and $\alpha_0 = 3/8 - (1/8)(ck_0)^2/(\omega_0^2 - \omega_p^2/4)$ is due to relativistic and nonlinear plasma wave effects. The term proportional to $(3/8)Ra_0^2$ in the dispersion relation represents the nonlinear effects of the bound electrons and can be substantially greater then the plasma term $\alpha_0 a_0^2 \cong a_0^2/4$. The resonant term in the expression for α_0, i.e., the term proportional to $(\omega_0^2 - \omega_p^2/4)^{-1}$, is due to the nonlinear plasma wave at frequency and wave number $(2\omega_0, 2k_0)$. In the present model propagation slightly below the plasma frequency is possible and is a result of the partial cancellation of the linear plasma current by the nonlinear polarization current of the bound electrons. Propagation far below the plasma frequency, however, can be achieved by canceling the linear plasma current with a nonlinear plasma current induced by the beating of two electromagnetic fields. This is referred to as electromagnetically induced transparency in plasmas [18].

To analyze the instabilities, we solve Eq. (2) together with the equation for δn_p to order $a_0^2\hat{a}_\pm$ giving

$$\begin{aligned}&\{D_+ - \Omega_0^2[c^2(k^2 + k_\perp^2)/D - 1 - (3/2)R(2(\omega_0 + \omega)^2 - \omega_0^2)/\omega_0^2]\}\\ &\quad\times\{D_- - \Omega_0^2[c^2(k^2 + k_\perp^2)/D - 1 - (3/2)R(2(\omega_0 - \omega)^2 - \omega_0^2)/\omega_0^2]\}\\ &\qquad = \Omega_0^4[c^2(k^2 + k_\perp^2)/D - 1 - (3/2)R(\omega_0^2 - \omega^2)/\omega_0^2]^2,\end{aligned} \tag{3}$$

where $D_\pm = \eta_0^2\omega^2 - c^2(k^2 + k_\perp^2) \pm 2(\eta_0^2\omega_0\omega - c^2k_0k)$, $\Omega_0^2 = \omega_p^2 a_0^2/4$, and $D = \omega^2 - \omega_p^2$. In the limit $R \rightarrow 0$, Eq. (3) reduces to previous results [12]. Because of the assumed polarizations of the pump and sideband waves, the two plasmon decay $(2\omega_p)$ instability is not described by the dispersion relation, Eq. (3).

The presence of bound electrons in a partially stripped plasma can result in an AMI which can completely dominate both the conventional RMI and FRS when $R \gg 1$. For $k_\perp = 0$, the AMI growth rate is

$$\Gamma = (ck\omega_p^2/2\omega_0^2)[(1 + 3R/2)a_0^2/2 - (ck/\omega_0)^2]^{1/2}, \tag{4}$$

and extends from $k = 0$ to $k = k_{\max} = (\omega_0 a_0/\sqrt{2}\,c)(1 + 3R/2)^{1/2}$ and peaks at $k = k_{\max}/\sqrt{2}$. Since the range of wave numbers over which the AMI exist is broad, it will be less sensitive to laser incoherence or plasma in homogeneities than the RMI or FRS. The maximum AMI growth rate is given by $\Gamma = (\omega_p^2 a_0^2/8\omega_0)(1 + 3R/2)$. Note that the maximum growth rate for the conventional RMI ($R = 0$) [10,12] is $\Gamma = \omega_p^2 a_0^2/8\omega_0$ and occurs at $k = \omega_0 a_0/2c \ll k_{\max}$. The ratio of the maximum growth rate for the AMI to the conventional RMI is $1 + 3R/2$, which can be much greater than unity. In the limit $n_p \to 0$, Eq. (4) implies that $k_{\max} \to \infty$ and, for finite k, the AMI growth rate scales as $\Gamma \sim n_p^{1/2} \to 0$. Hence, the AMI is stable in the absence of a plasma. The physical mechanism for the AMI is due to anomalous GVD that is provided by the plasma electrons, and self-phase modulation that results from the nonlinearities associated with the bound electrons [19]. The GVD due to bound electrons can be neglected compared to that of the free electrons. GVD is measured by the parameter [19] $\beta_2 = c^{-1}\partial^2(\omega_0\eta)/\partial^2\omega_0$. The plasma contribution to β_2 is $\beta_{2p} = -\omega_p^2/c\omega_0^3 \cong -10^{-28}\ \mathrm{sec}^2/\mathrm{cm}$ (for $\omega_0/\omega_p \cong 10$ and $\lambda_0 \cong 1\ \mu$m) and is typically opposite in sign and 10^3 times greater in magnitude than the contribution from usual gases at STP. Plasma waves do not play a role in the AMI.

The growth rate for the FRS instability (for $k_\perp = 0$) peaks at $k = \omega_p/c$ and is distinct from the AMI instability for $Ra_0^2 < (4/3)\omega_p^2/\omega_0^2$. For $Ra_0^2 \ll (4/3)\omega_p^2/\omega_0^2$ the FRS growth rate at $k = \omega_p/c$ is given by the conventional expression [12–14], $\Gamma = \omega_p^2 a_0/2^{3/2}\omega_0$. As Ra_0^2 increases and approaches $(4/3)\omega_p^2/\omega_0^2$ the two instability growth rates merge. For $Ra_0^2 \gg (4/3)\omega_p^2/\omega_0^2$ the FRS instability is dominated by the AMI. The ratio of the maximum growth rate for the AMI to the conventional FRS instability is $(3\sqrt{2}/8)Ra_0$. The Raman backscatter instability, on the other hand, is unaffected by the presence of bound electrons.

The filamentation instability can also be strongly affected by bound electrons. Taking $k = 0$, the AFI growth rate is

$$\Gamma = (ck_\perp\omega_p/2\omega_0)\,[(1 + 3R/2)a_0^2/2 - (ck_\perp/\omega_p)^2]^{1/2}, \tag{5}$$

and extends from $k_\perp = 0$ to $k_\perp = k_{\perp\max} = (\omega_p a_0/\sqrt{2}\,c)(1 + 3R/2)^{1/2}$ and peaks at $k_\perp = k_{\max}/\sqrt{2}$. The maximum growth rate for the AFI is $\Gamma = (\omega_p^2 a_0^2/8\omega_0)(1 + 3R/2)$, which is identical to the maximum AMI growth rate. For $R = 0$, the growth rate of the conventional RFI for a plasma is recovered [10,12], whereas for $R \gg 1$, the growth rate of the conventional filamentation instability for a neutral gas is recovered [17]. The ratio of the peak AFI growth rate to the peak RFI growth rate is $1 + 3R/2$, which can be much greater than unity. The effect of the AFI is to transversely break up the laser pulse into filaments, each having a transverse dimension $r_\perp \cong 2/k_\perp$ and a power per filament roughly equal to the critical power. The power per filament is $P = I\pi r_\perp^2 \cong I(4\pi/k_\perp^2) \cong P_p/(1 + 3R/2) \cong P_a$, where $k_\perp = (\omega_p a_0/2c)(1 + 3R/2)^{1/2}$ corresponds to the maximum growth rate. This model assumes that the transverse dimension of the laser pulse is greater than $r_\perp$. For the filamentation instability ($k = 0$), the sideband frequency is purely imaginary, i.e., $\omega^2 < 0$. The instability, therefore, is purely growing in time and does not propagate transversely out of the laser pulse. Plasma waves are not excited in the AFI for $k = 0$.

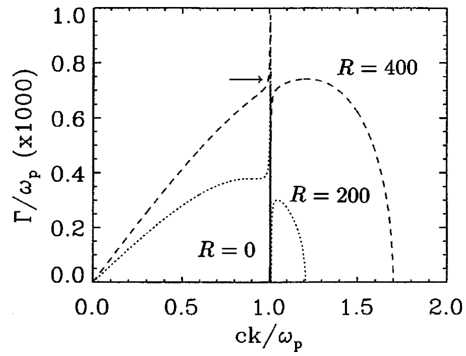

FIG. 1. Normalized modulation growth rate, Γ/ω_p, versus normalized longitudinal wave number, ck/ω_p, for $\omega_0/\omega_p = 10$, $a_0 = 0.01$, and $R = 0$ (solid curve), $R = 200$ (dotted curve), and $R = 400$ (dashed curve), where $k_\perp = 0$. The amplitude of the FRS peak for $R = 0$ is indicated by an arrow.

Growth rates from solutions of Eq. (3) are shown in Figs. 1–3 for $a_0 = 0.01$ ($I = 1.4 \times 10^{14}\ \mathrm{W/cm}^2$ for $\lambda_0 = 1\ \mu$m) $\omega_0/\omega_p = 10$ ($n_p \cong 10^{19}\ \mathrm{cm}^{-3}$ for $\lambda_0 = 1\ \mu$m) and various values of the effective R ranging from 0 to 400. In these figures the growth rates and wave numbers are normalized to ω_p and ω_p/c, respectively. Figure 1 shows the modulational growth rate ($k_\perp = 0$) for $R = 0$, 200, and 400. Figure 2 shows the filamentation growth rate ($k = 0$) for $R = 0$, 200, and 400. Figures 3(a) and 3(b) show the growth rates as a function ck/ω_p and $ck_\perp/\omega_p$ for (a) $R = 0$ and (b) $R = 400$, respectively, where $a_0 = 0.01$ and $\omega_0/\omega_p = 10$. The

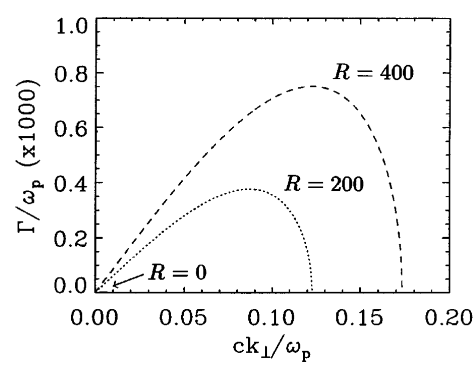

FIG. 2. Normalized filamentation growth rate, Γ/ω_p, versus normalized transverse wave number, $ck_\perp/\omega_p$, for $\omega_0/\omega_p = 10$, $a_0 = 0.01$, and $R = 0$ (solid curve), $R = 200$ (dotted curve), and $R = 400$ (dashed curve), where $k = 0$. The $R = 0$ growth rate is not discernible on this scale.

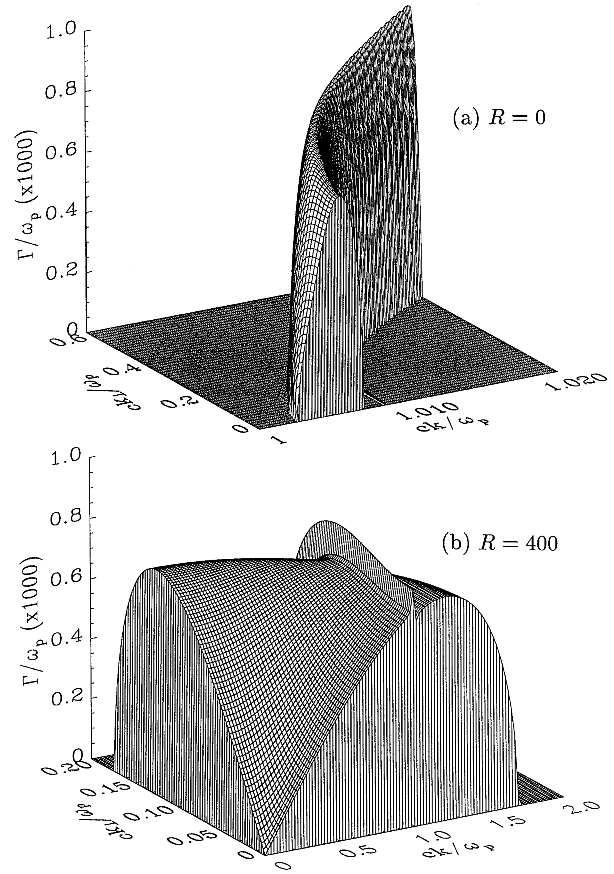

FIG. 3. Surface plots of normalized growth rate as a function ck/ω_p, and $ck_\perp/\omega_p$, for (a) $R = 0$ and (b) $R = 400$, where $a_0 = 0.01$, $\omega_0/\omega_p = 10$. Note the change in scale in (a) and (b).

$R = 0$ curves correspond to the conventional results for a fully stripped plasma. Figure 1 shows the conventional ($R = 0$) FRS growth rate, which has a maximum of $\Gamma/\omega_p \cong 7.2 \times 10^{-4}$ and is narrowly peaked about $ck/\omega_p \cong 1$, however, the conventional RMI growth rate, which has a maximum of $\Gamma/\omega_p \cong 1.3 \times 10^{-6}$ at $ck/\omega_p \cong 5 \times 10^{-2}$, is not discernible on this plot. Similarly, the conventional ($R = 0$) RFI growth rate, which has a maximum of $\Gamma/\omega_p \cong 1.3 \times 10^{-6}$ at $ck_\perp/\omega_p \cong 5 \times 10^{-3}$, is not discernible in Fig. 2. Figure 3(a) shows the conventional Raman forward and side-scatter growth rates peaked near $ck/\omega_p \cong 1$ (the RFI and RMI growth rates are not discernible on this scale). For $R \gg 1$, the growth rates of the AMI, AFI, and FRS instability are significantly enhanced. For $R \gg 1$, Fig. 1 (Fig. 2) shows the AMI (AFI) growth rate rising from zero at $k = 0$ ($k_\perp = 0$), reaching a maximum at $k \cong k_{\max}/\sqrt{2}$ ($k \cong k_{\perp\max}/\sqrt{2}$), and decreasing to zero at $k \cong k_{\max}$ ($k_\perp \cong k_{\perp\max}$). Figure 3(b) shows the growth rates as functions of k and $k_\perp$ for $R = 400$ and indicates that the maximum growth rates for the AMI and AFI are approximately equal. The growth rate of the Raman instability near $ck/\omega_p \cong 1$ is also enhanced. Note that the Raman peak in Fig. 3(b) is not fully resolved due to the coarse grid used in the surface plot.

One of us (P. S.) would like to thank S. E. Harris for many stimulating and useful discussions. The authors also acknowledge useful conversations with J. Reintjes, A. Ting, R. Lehmberg, P. Shkolnikov, G. Joyce, and S. Bodner. This work was supported by the Office of Naval Research and the Department of Energy.

*Present address: Icarus Research, Inc., P.O. Box 30780, Bethesda, MD 20824-0780.

[1] S. Suckewer and C.H. Skinner, Science **247**, 1553 (1990); D.C. Eder *et al.*, Phys. Plasmas **1**, 1744 (1994); B.E. Lemoff *et al.*, Phys. Rev. Lett. **74**, 1574 (1995); P. Eisenberger and S. Suckewer, Science **274**, 201 (1996).
[2] M. Tabak *et al.*, Phys. Plasmas **1**, 1626 (1994); N.D. Delamater *et al.*, Phys. Plasmas **3**, 2022 (1996); C.J. Pawley *et al.*, Phys. Plasmas **4**, 1969 (1997).
[3] P. Sprangle *et al.*, Phys. Lett. **53**, 2146 (1988); P. Sprangle *et al.*, Phys. Rev. Lett. **64**, 2011 (1990); P. Sprangle *et al.*, Phys. Rev. Lett. **69**, 2200 (1992); E. Esarey *et al.*, IEEE Trans. Plasma Sci. **PS-24**, 252 (1996).
[4] C.E. Clayton *et al.*, Phys. Plasmas **1**, 1753 (1994); A. Modena *et al.*, Nature (London) **377**, 606 (1995); D. Umstadter *et al.*, Science **273**, 472 (1996); A. Ting *et al.*, Phys. Plasmas **4**, 1899 (1997).
[5] J. Macklin, J. Kmetec, and C. Gordon, Phys. Rev. Lett. **70**, 760 (1993); J. Zhou *et al.*, *ibid.* **76**, 752 (1996).
[6] P. Sprangle and E. Esarey, Phys. Rev. Lett. **67**, 2021 (1991); E. Esarey *et al.*, IEEE Trans. Plasma Sci. **21**, 95 (1993).
[7] H.M. Milchberg *et al.*, Phys. Plasmas **3**, 2149 (1996); Y. Ehrlich *et al.*, Phys. Rev. Lett. **77**, 4186 (1996); P. Sprangle and E. Esarey, Phys. Fluids B **4**, 2241 (1992).
[8] X. Liu and D. Umstadter, in *Short Wavelength V: Physics with Intense Laser Pulses,* edited by M.D. Perry and P.B. Corkum (Optical Society of America, Washington, DC, 1993), P. 45; A. Braun *et al.*, Opt. Lett. **20**, 73 (1995).
[9] P. Sprangle, E. Esarey, and J. Krall, Phys. Rev. E **54**, 4211 (1996).
[10] C.E. Max, J. Arons, and A.B. Langdon, Phys. Rev. Lett. **33**, 209 (1974).
[11] A.L. Berkhoer and V.E. Zakharov, Sov. Phys. JETP **31**, 486 (1970).
[12] J. McKinstrie and R. Bingham, Phys. Fluids B **4**, 2626 (1992).
[13] J.F. Drake *et al.*, Phys. Fluids **7**, 778 (1974); K. Estabrook and W.L. Kruer, Phys. Fluids **26**, 1892 (1983); W.B. Mori *et al.*, Phys. Rev. Lett. **72**, 1482 (1994).
[14] T.M. Antonsen, Jr. and P. Mora, Phys. Rev. Lett. **69**, 2204 (1992); Phys. Fluids B **5**, 1440 (1993).
[15] A.G. Litvak, Zh. Eksp. Teor. Fiz. **57**, 629 (1969) [Sov. Phys. JETP **30**, 344 (1969)].
[16] G. Schmidt and W. Horton, Comments Plasma Phys. **9**, 85 (1985); P. Sprangle, C.M. Tang, and E. Esarey, IEEE Trans. Plasma Sci. **PS-15**, 145 (1987); G.Z. Sun *et al.*, Phys. Fluids **30**, 526 (1987).
[17] J.F. Reintjes, *Nonlinear Optical Parametric Processes in Liquids and Gases* (Academic, Orlando, FL, 1984).
[18] S.E. Harris, Phys. Rev. Lett. **77**, 5357 (1996).
[19] G.P. Agrawal, *Nonlinear Fiber Optics* (Academic, San Diego, 1995).